Dynamics of defects in parametrically excited capillary ripples

A. B. Ezersky, D. A. Ermoshin, and S. V. Kiyashko
Institute of Applied Physics, Russian Academy of Science, 46 Uljanov Street, 603600 Nizhny Novgorod, Russia
(Received 20 June 1994)

Investigations of parametrically excited capillary ripples—a perfect structure consisting of two mutually orthogonal pairs of standing waves—reveal that two topological defects of the same sign belonging to the waves, traveling in opposite directions in one pair, may form a stable bound state. Individual dislocations in the form of such bound states may interact with each other, the interaction being the most effective if they consist of defects belonging to one pair. It is shown that the dislocations may either annihilate, if they have opposite topological charges, or are arranged into quasistable states in the form of a linear chain, in the case of like topological charges.

PACS number(s): 47.35.+i, 64.60.Cn, 47.20.−k

I. INTRODUCTION

Parametrically excited capillary ripples have been intensively investigated, in particular, in analysis of pattern formation and the transition to chaos. Depending on parameters of a liquid, spectral composition, and amplitude of a pump field on the surface of a horizontal liquid layer vibrating vertically, different perfect structures in the form of squares, hexahedrons [1], or the so-called quasistructures [2,3], which are macroscopic analogs of quasicrystals in solid state physics, may be observed in spatially extended systems.

The dynamics of the square structures formed by two mutually orthogonal pairs of standing capillary waves [4,5] that appear in a broad range of the parameters of a liquid was investigated in ample detail. It was found [5] that modulation waves arise against the background of a square lattice even at a slight excess over the threshold of parametric instability. A further increase in the amplitude of the pump field leads to an intensification of the envelope waves and to the transition from regular patterns to spatiotemporal chaos.

However, modulation waves exist in the liquid layers whose depth is greater than the wavelength of capillary waves. If the layer is sufficiently thin, which is indicative of strong energy dissipation in the boundary layer of capillary waves at the bottom, no modulation waves are observed. In this case, irregularities in the lattice formed by capillary waves may be associated with the emergence of chains of dislocations at the boundaries of the domains, i.e., the regions with a perfect field structure. For instance, it was revealed in [6] that in rather thin layers of a liquid the transition from an initially irregular state to a perfect square lattice occurs through formation on the liquid surface of an ensemble of domains. The transition to a perfect structure may be represented as a process of domain collapse or merging. Typical features of this process were recently analyzed in [6].

In this paper we investigate the dynamics of an individual dislocation, its fine structure, as well as elementary acts of interaction of the dislocations. Until recently dynamics of dislocations was investigated primarily in systems without propagating perturbations, namely, in liquid crystals [7–9] or in liquids with convection [10,11]. We believe that the dynamics of dislocations in capillary ripples differs from that in the systems enumerated above because, in the case of parametric excitation, the structures are formed as a result of interaction of the wave propagating in a spatially homogeneous oscillating field. No theoretical calculations of the dynamics of dislocations in such fields are available yet, therefore experimental investigation is of particular significance.

II. EXPERIMENT

Experiments were performed on capillary ripples parametrically excited on the surface of a liquid poured into a circular cavity 157 mm in diameter. Silicon oil ПМС-5 with kinematic viscosity $\nu=0.05$ cm^2/s, density $\rho=0.89$ g/cm^3, and surface tension coefficient $\sigma=17$ dyn/cm was taken as an operating liquid. (All the data are given for the temperature of 25 °C.) The choice of silicon oil as an operating liquid is explained by its low evaporability and resistance to surface contamination.

Vertical vibrations of the cavity (see Fig. 1) were produced by the Brul & Kjar 4805 vibrostand which was fed by sinusoidal voltage through the Brul & Kjar 2707 power amplifier. A test generator built into the Brul & Kjar 2034 spectrum analyzer was used as a source of sinusoidal voltage. The amplitude of amplification of vertical vibrations of the cavity was measured by means of the KD29 piezoaccelerometer fabricated by VEB Metra Beβ und Frequenztechnik Radebeul. The signal from KD29 was transmitted through the Brul & Kjar 2035 preamplifier to the spectrum analyzer. Such a procedure enabled us to control not only the amplitude of the pump field but also its spectral composition.

The image of capillary ripples was recorded by a video camera placed at a distance of about 130 cm from the surface of the cavity. Six low-power incandescent lamps arranged around the objective of the video camera provided sufficiently uniform illumination of the surface of capillary ripples.

In analyzing the videotape obtained in the experiment

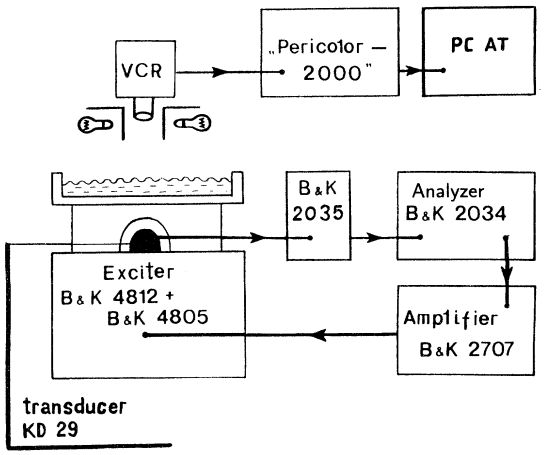

FIG. 1. Scheme of experiment. VCR is a video camera recorder and PC AT is an AT-type personal computer. A Brul & Kjar Model 2035 preamplifier and a Model Pericolor 2000 image processor are also shown.

sequences of pictures were frame-grabbed by means of "Pericolor 2000," a system for image processing coupled to a personal computer.

A. Image processing

Investigation of the dynamics of individual dislocations necessitates a regular procedure allowing for their identification in the fields of brightness of capillary ripples. To this end, one needs, first of all, to determine the complex amplitude of capillary ripples. We did it following the procedure proposed in [7], which dynamics of defects in one-dimensional rolls appearing at electrohydrodynamic convection in liquid crystals was investigated.

The two-dimensional Fourier spectrum was determined by the field of image brightness. For the square lattice formed by two mutually orthogonal pairs of counterpropagating waves, this spectrum is a set of spikes. It is worthy of notice that by virtue of the inertia of a video camera, the image of parametrically excited capillary ripples is averaged in time. The relationship between surface deviation η and changes of the image brightness δI was broadly discussed in the literature and we omit it here. We only note that to the first approximation one can take $\delta I \sim \langle \eta^2 \rangle$. Then, for two pairs of standing capillary waves whose wave vectors are oriented along the $0X$ and $0Y$ axes, $a\cos(\omega t)\cos(kx)$ and $b\cos(\omega t)\cos(ky)$, the spectrum of image brightness consists of the spatial harmonics with wave vectors $\mathbf{K}_x=(\pm 2k,0)$, $\mathbf{K}_y=(0,\pm 2k)$, $\mathbf{K}'_{x,y}=(\pm k,\pm k)$, and $\mathbf{K}_{x,y}=(\pm k,\mp k)$. The amplitudes of these spatial harmonics are proportional to the following parameters: $A(\mathbf{K}_x)\sim a^2$, $A(\mathbf{K}_y)\sim b^2$, and $A(\mathbf{K}_{x,y})$, $A(\mathbf{K}'_{x,y})\sim ab$. In order to obtain information about capillary waves in each mutually orthogonal pair we filtered in the spectrum of image brightness the harmonics in the neighborhood of spectral peaks $(\pm 2k,0)$ and $(0,\pm 2k)$. From these harmonics in the neighborhood of each peak we calculated

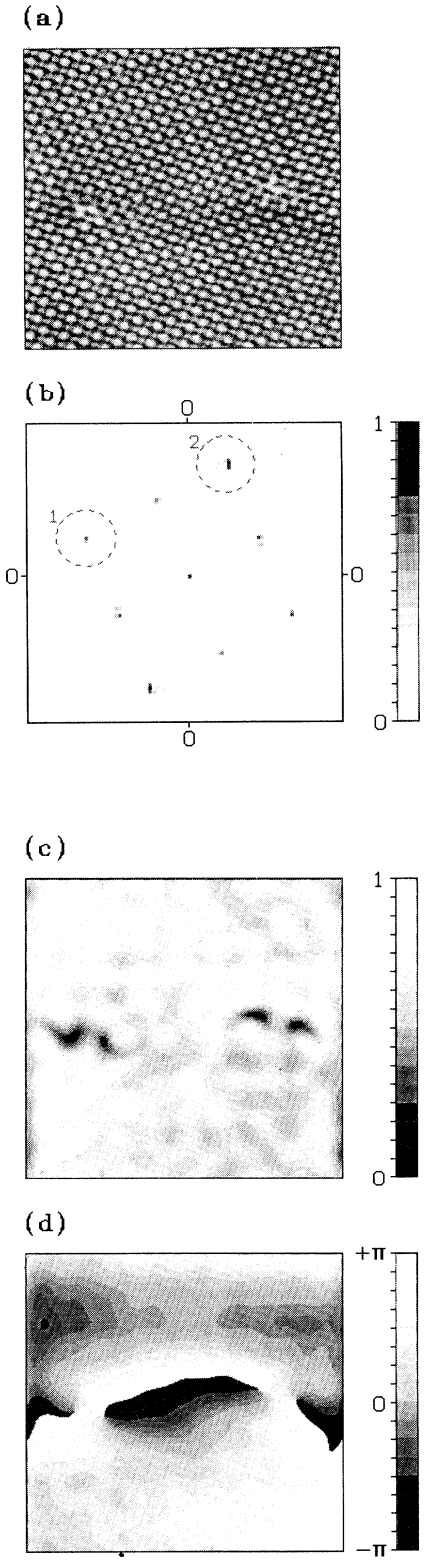

FIG. 2. (a) Field of capillary ripples. (b) Fourier spectrum. The dashed lines mark the spectral peaks for which the envelope fields were investigated. (c) Field of the amplitude of envelope for spectral peak 1. (d) Field of the phase of envelope for spectral peak 1.

the inverse Fourier transform supposing that the centroid for all the harmonics belonging to the transmission band of the filter is a zero spatial frequency. In this fashion we determined the envelopes of capillary waves.

An example for determination of a complex amplitude is presented in Fig. 2. The brightness field of capillary ripples shown in Fig. 2(a) has two dislocations. The Fourier spectrum calculated by this field of brightness containing 256×256 points is given in Fig. 2(b). The inverse Fourier transform was performed in the neighborhood of the spectral peaks shown by the dashed circles in Fig. 2(b) for 16×16 harmonics. The field for the amplitude of the envelope obtained in the calculations of the inverse Fourier transform from the harmonics in region 1 is presented in Fig. 2(c) and the phase field in Fig. 2(d). One can see from these figures that each dislocation contains two point defects slightly spaced apart. These two defects have like topological charges while the dislocations on the left and on the right of Fig. 2(d) have opposite charges, -4π and $+4\pi$, respectively. (It is assumed that the direction of increasing phase is counterclockwise.) The minima of the amplitudes of the envelopes depicted in Fig. 2(c) were taken as the positions of the defects. The field amplitude was almost zero at these points.

The two dislocations in the field of capillary ripples given in Fig. 2(a) belong to one wave pair. Calculations of the inverse Fourier transforms by region 2 [see Fig. 2(b)] demonstrate that the envelope field contains no dislocations. Neither amplitude decrease down to zero nor integral phase advance in the path tracing around a closed contour are observed at the site of expected defects. Note that in our experiments we also observed dislocations belonging to different pairs of capillary waves. By determining the envelopes of all harmonics we readily identified the location of dislocations in these cases too.

B. Results of experiment

Dislocations in a regular lattice formed by standing capillary waves were observed in a rather broad interval of liquid layer thicknesses and frequencies and amplitudes of the pump field. (The region of the existence of such dislocations was investigated in [6].) The dynamics of solitary dislocations was observed in experiments on a liquid layer of thickness $h=0.5$ mm; the external force frequency f was taken to be 100 Hz, and supercriticality ε was varied in a narrow region about 0.5 ($\varepsilon=G/G_0-1$, where G is the amplitude of acceleration of the pump field and G_0 is the threshold value at which parametric generation occurs).

On formation of a perfect structure (this process was investigated in [6]) for the parameters specified above, dislocations appeared every now and then near the walls of the cavity and performed rather complicated motions all over the cavity until they escaped at the wall. Owing to the fact that the mutually orthogonal pairs of waves forming the square lattice contacted a circular wall, the side boundary was a source of defects. It should be emphasized that, in the region of the parameters investigated in our experiment, the capillary ripples were immune to spontaneous birth of dislocations. We did not observe the birth of dislocations far from the walls, except for the cases when we produced large-amplitude perturbations in the layer (for example, by stirring the liquid inside a region of about 5×5 wavelengths).

Each elementary dislocation consisted of two defects having like topological charges (Fig. 2). One can see from Fig. 2 that the defects in each dislocation are displayed by a distance $d_{1,2}$ relative to one another, primarily, along the direction of wave propagation in the pair. Measurements at different frequencies and supercriticalities showed that the distance $d_{1,2}$ amounted to 1.5–2.5 wavelengths.

Since the emergence of dislocations near the walls was a random process, we were able to resolve the instants of time when there were only two dislocations in the cavity. This enabled us to observe elementary acts of interaction of the dislocations belonging to different pairs or to one wave pair. The dislocations could annihilate when they had opposite topological charges and belonged to one wave pair. The trajectories of the defects in such dislocations are shown in Fig. 3(a). The change of the distance $d_{1,2}$ between the dislocation cores in time is demonstrat-

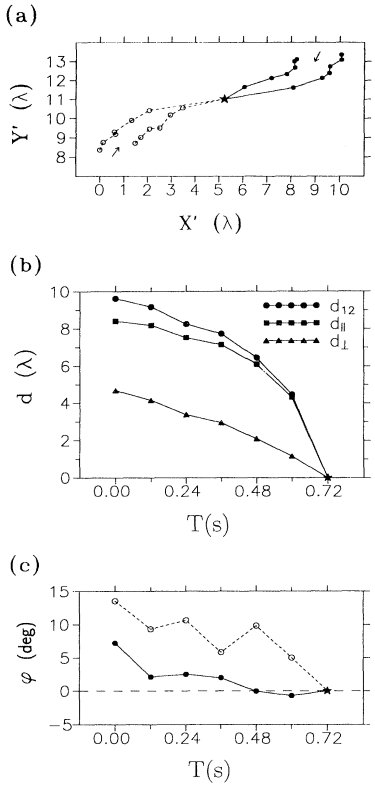

FIG. 3. Annihilation of dislocations for $\varepsilon=0.5$ and $f=100$ Hz: (a) trajectories of dislocations, X and Y are measured in wavelengths; (b) distance between the dislocation cores (curve $d_{1,2}$), projection of the distance onto the direction of wave propagation in the pair (curve $d_{\parallel}$), and projection onto the trasversal direction (curve $d_{\perp}$); (c) the angle between the direction of wave propagation in the pair and the line connecting the points of defect location.

ed in Fig. 3(b). The dislocation core is understood as the arithmetic mean of the position of the defects forming the dislocation. The curve $d_{\parallel}$ corresponds to the projection of the distance onto the direction of wave propagation, and the curve $d_{\perp}$ onto the perpendicular direction. Thus, in this example of annihilation the dislocations primarily glide, i.e., the defects move across the capillary wave fronts and, besides, the velocity of reprochement increases with decreasing distance between the dislocations. A perfect structure is born after annihilation of the dislocations.

Experiment verifies that such a complete annihilation is a rather typical process. However, we also observed, if only very rarely, collisions of the dislocations belonging to one wave pair and having opposite charges that gave rise to the birth of dislocations with opposite topological charges in the other wave pair. (Only two such interactions were registered in the six-hour recordings of the experiment.) An example of such a process is demonstrated in Figs. 4(a) and 4(b). The trajectories of motion are drawn in Fig. 4(a). During collision, one of the defects belonging to the left dislocation annihilates with the defect that has the opposite charge and belongs to the right dislocation at the point marked by the asterisk. Two other defects (marked by R and L) with opposite charges are spaced approximately 6λ apart. As they approach each other from the sites marked by the dots, dislocations are born in the orthogonal wave pair. It is worthy of notice that defect orientation relative to the capillary wave fronts in each dislocation remains almost unchanged in the course of collisions. In Fig. 4(b), the curves $d_{1,2}$ and $d'_{1,2}$ correspond to the distances between the dislocation cores in mutually orthogonal pairs, while the curves $d_{\perp}$

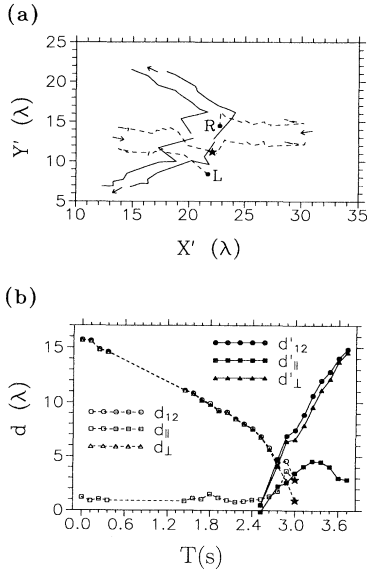

FIG. 4. Collision of dislocations with opposite topological charges giving rise to the birth of a pair of dislocations in the orthogonal wave pair for $\varepsilon=0.50$ and $f=102$ Hz: (a) trajectories of dislocations; (b) distances between merging and appearing dislocations.

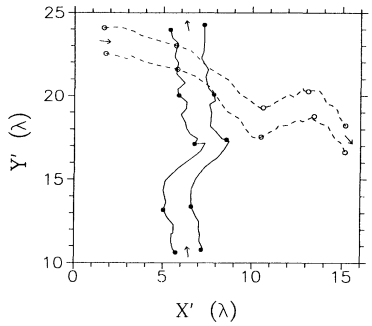

FIG. 5. Trajectories of interacting dislocations belonging to different wave pairs for $\varepsilon=0.56$ and $f=103$ Hz.

and $d'_{\perp}$ and the curves $d_{\parallel}$ and $d'_{\parallel}$ correspond to the projections of the distance between the cores in the transversal and parallel directions of wave propagation, respectively. The dashed curves mark the distance between the dislocations prior to collision, and the solid curves represent that after collision. Clearly, the dislocations climb prior to collision, i.e., move along the wave fronts.

The dislocations belonging to different wave pairs interacted rather weakly. This process is demonstrated in Fig. 5. Such dislocations could even go through each other and no significant changes in their trajectories of motion would occur. A small slowing down of the relative motion of the dislocations was observed when they were very close to each other, but we failed in making quantitative measurements.

Besides pairlike interactions of dislocations we investigated the interaction of several individual dislocations. Observations reveal that interaction of the dislocations having like charges and belonging to one wave pair may give rise to a linear chain of dislocations in the lattice. Such a chain is depicted in Fig. 6(a). The same image but on filtering and setting a contrast is given in Fig. 6(b). Experiment shows that for the chain to be formed a localized source of dislocations generating defects of the same

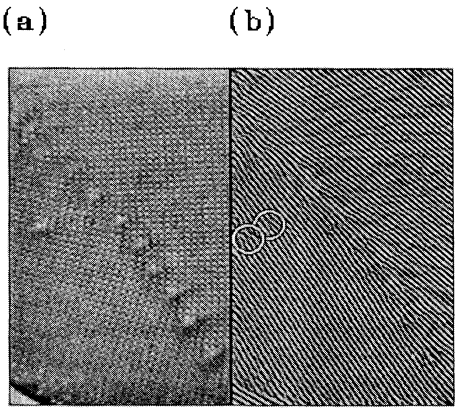

FIG. 6. Linear chain of dislocations for $\varepsilon=0.47$ and $f=102$ Hz: (a) image of capillary ripples; (b) filtered and contrasted image of a single wave pair.

sign is needed. In the absence of such a source, the probability of appearance of a sufficient amount of dislocations having the same sign in one pair is very low and no linear chain is formed as a rule. The source of dislocations may be localized due to the presence of solid particles at the wall of the cavity. The chain of dislocations presented in Fig. 6 was obtained when a piece of cotton thread was placed at the wall. A linear chain is formed as follows. Every now and then, a dislocation appears from the source of defects on the wall and climbs along the wave pair front. The dislocations tend to align along the wave fronts. The long-lived chains of dislocations always originate and end at the wall. The linear density of dislocations is rather uniform but the distance between them decreases from the walls to the center of the cavity. We called such a dislocation chain a domain wall [6]. One can see from Fig. 6(b) that the domain wall consists of the dislocations belonging to one wave pair only. It was revealed that there were no defects in the domain wall in the other wave pair. The wave fronts in it were only distorted near the domain wall but the number of wave fronts did not change in the transition across the domain wall. The wave pairs were mutually orthogonal on both sides of the domain wall.

How does a single dislocation interact with the domain wall? This depends on whether the dislocation belongs to the same wave pair as the dislocations constituting the domain wall or to the other wave pair. The first case is presented in Fig. 6. The dislocation that does not belong to the domain wall [the defects forming this dislocation are encircled in Fig. 6(b)] but belongs to the same wave pair is attracted by the domain wall. In the course of interaction of a cognate dislocation with the domain wall two processes may be observed: annihilation with one of the dislocations in the chain (when the dislocations in the domain wall and the individual dislocation have opposite topological charges) or building of the individual dislocation in the domain wall (when the dislocations have like topological charges). The distance between the dislocations in the domain wall increases when annihilation occurs and decreases when the dislocations build in the domain wall. In the second case, the dislocation belonging to the wave pair that no other dislocations belong to may go through the domain wall (see Fig. 7). To make the picture more illustrative we filtered the image of ripples so that there remained only the waves in which the defects form a domain wall. The location of the defects forming the dislocation belonging to the orthogonal wave pair at different instants of time is shown by crosses in Fig. 7. As the dislocation is moving across the wall, the other dislocations also change their relative position; as a result of this the wall bends (Fig. 7, picture 5). After the dislocation has crossed the domain wall, the latter almost recovers its original state.

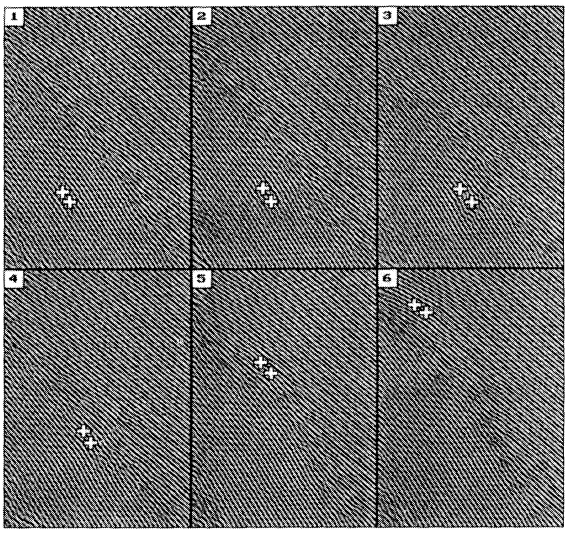

FIG. 7. Dislocations passing through the wall for $\varepsilon=0.47$ and $f=100$ Hz. Repetition rate for frames 1 and 2, 2 and 3 is 0.24 s, and for the other frames 0.12 s.

C. Discussion of results

The topological defects revealed in the experiment refer, strictly speaking, to image brightness fields. The relationship between the brightness field and the field of capillary waves is rather complicated, and frequently ambiguous. Therefore it is not a trivial task to reconstruct the field of capillary ripples immediately by its image. We can propose, however, models for the fields of capillary ripples which describe the distribution of image brightness observed in experiments. Let the waves

$$\eta=\tfrac{1}{2}[a_+\exp(ikx)+a_-\exp(-ikx)+b_+\exp(ikx) +b_-\exp(-iky)]\exp(-i\omega t)+\text{c.c.} \quad (1)$$

be excited on the surface of a liquid.

Suppose that the waves have equal amplitudes and phases $a_+=a_-=b_+=b_-=a$ and the wave propagating along the $0X$ axis contains a topological defect. The field of capillary ripples corresponding to this case is presented in the form [6]

$$\eta=a\{\cos(ky)+f(r)\cos[kx+\arctan(y/x)]\}\cos(\omega t)\ , \quad (2)$$

where $f(r)$ is the function $f=\tanh[\kappa(x^2+y^2)^{1/2}]$ vanishing to zero for $r=0$ and $f\to 1$ for $r\to\infty$.

As shown in [6], the distribution of the image brightness of capillary ripples, δI, for $\kappa\sim k$ resembles the image of a single dislocation recorded in experiment assuming that

$$\delta I\sim\langle\eta^2\rangle\ . \quad (3)$$

Calculations of the complex amplitude of the image of capillary ripples specified in (2) show that the fields $|A|$ and φ differ from those obtained in experiment. The principal difference is that the defect with topological charge 4π is located at the point $x=0$, $y=0$ of the image brightness of capillary ripples. It was revealed in experiment that each dislocation consists of two 2π topological charges located along the direction of wave propagation in the pair. This suggests that a good agreement between experiment and model may be obtained if we assume that

the dislocation consists of two defects belonging to the waves traveling in opposite directions. Under this assumption the capillary wave field may be written in the form

$$\eta=\frac{a}{2}(\cos(\omega t-ky)+\cos(\omega t+ky)+\tanh\{\kappa[(x-x_1)^2+(y-y_1)^2]^{1/2}\}\cos\{\omega t+kx+\arctan[(y-y_1)/(x-x_1)]\}$$
$$+\tanh\{\kappa[(x-x_2)^2+(y-y_2)^2]^{1/2}\}\cos\{\omega t-kx-\arctan[(y-y_2)/(x-x_2)]\})\ . \quad (4)$$

The field (4) transforms into (2) if we set $x_{1-1}=0$ and $y_{1-2}=0$.

We note that only the dislocations consisting of pairs of defects were observed in our experiment. Such a pair of defects, evidently, forms a state possessing a considerable reserve of stability due to strong coupling of the capillary waves propagating in opposite directions in a spatially uniform pump field. As follows from the experiment, the distance $d_\parallel$ between the defects along the direction of wave propagation amounts to about $(1.5-2.5)\lambda$ (where λ is the wavelength of perturbations), and in the transverse direction it is $d_\perp\sim(0-0.5)\lambda$. Such a distance between defects is typical of both a single dislocation (Fig. 2) and the dislocations forming a linear chain (Figs. 6 and 7), i.e., a domain wall. The domain boundary is a double row of defects.

We now consider the simplest theoretical model of a domain wall for parametrically excited ripples. The equations for slowly varying complex amplitudes of pairs of capillary ripples parametrically excited on the surface of a liquid were considered in [4]. It was ascertained that the envelope waves in mutually orthogonal pairs interact only weakly, therefore the equations for amplitudes in each pair can be investigated independently. For slowly varying amplitudes $a_\pm$ of the waves propagating along the $0X$ axis, regarding the coefficients of nonlinear wave interaction to be purely real (there is no linear damping), and restricting the consideration to a stationary case (the amplitudes a are time independent), we have [4]

$$\mp v_g\frac{\partial a_\pm}{\partial x}-v_g\frac{i}{2k}\frac{\partial^2 a_\pm}{\partial y^2}=\gamma a_\pm-iHa_\mp^*+i\Delta a_\pm$$
$$+ia_\pm(T|a_\pm|^2+S|a_\mp|^2)\ . \quad (5)$$

Here v_g is the group velocity of the waves, γ is the capillary wave damping, H is the coefficient of interaction with the pump field, S and T are the coefficients of nonlinear wave coupling, and Δ is falling out of exact synchronism with pump frequency.

For real amplitudes $A_\pm$ and phase $\Phi=\varphi_+ +\varphi_-$, where

$$a_\pm=A_\pm\exp(\pm i\kappa_y y)\exp(i\varphi_\pm)\ , \quad (6)$$

the equations of motion reduce to the form [4]

$$v_g\frac{\partial A_+}{\partial x}=-\gamma A_+ +HA_-\sin\Phi\ ,$$
$$v_g\frac{\partial A_-}{\partial x}=\gamma A_- -HA_+\sin\Phi\ , \quad (7)$$
$$\frac{\partial\Phi}{\partial x}=\left[\frac{A_-}{A_+}-\frac{A_+}{A_-}\right]H\cos\Phi+(S-T)(A_+^2-A_-^2)\ .$$

Note that the parameter κ_y does not enter into the system (7) which has the integral of motion $A_+A_-\cos\Phi+rA_+^2A_-^2=\text{const}$, where $r=(T-S)/2H$.

The system (7) on a phase plane was investigated to the full extent in [4]. It was shown, in particular, that it has a separatrix, the motion along which corresponds to the transition from the equilibrium state $A_+=A_-=A_0$ to the equilibrium state $A_+=A_-=-A_0$ where

$$A_0=\left[\frac{4(H^2-\gamma^2)}{(S-T)^2}\right]^{1/4}\ . \quad (8)$$

Such a separatrix is presented in Fig. 8 for $\varepsilon=(H-\gamma)/\gamma=0.5$, $r=1500$ 1/cm^2, and the damping coefficient for capillary waves $\gamma=30$ s^{-1}. The distance along the $0X$ axis is taken in wavelengths. The points at which the amplitudes A_+ and A_- of the envelope waves turn to zero are at a distance of $\Delta x\sim 2$. This is in a good agreement with the data of experiment (see Fig. 6) if the distances between these points in the one-dimensional model (7) are compared with the distance between the defects in each dislocation. Note that, according to calculations, the distance between Δx depends rather weakly on the parameter r (when the latter changes by three orders of magnitude while Δx remains practically unchanged) and is determined, primarily, by wave damping γ and supercriticality ε.

The presence of a free parameter $\kappa_y\neq 0$ allows us to obtain in the frames of this model the domain walls located at a small angle to the fronts of capillary waves. Note that a zero density of dislocations should correspond to

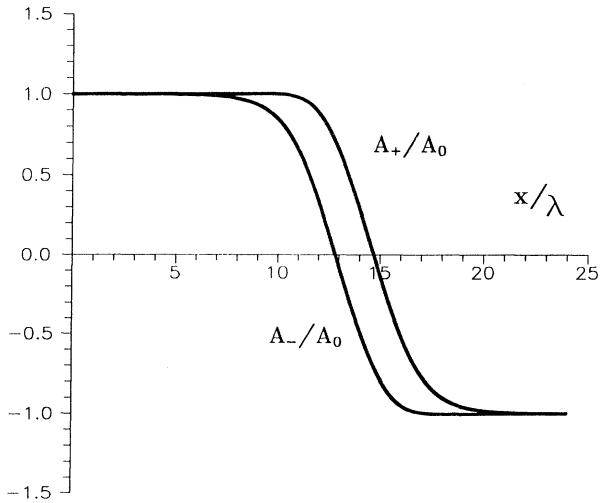

FIG. 8. Variation of the wave amplitude in a domain wall.

such domain walls in experiment because the fronts in the pair of capillary waves (6) do not change their orientation in the transition through such a domain wall.

The change of wave front orientation and emergence of defects are described by the solution of (7) that transforms to $a_{\pm}=A_0\exp(\pm i\kappa_y y)\exp(i\varphi_{\pm})$ for $x\rightarrow-\infty$ and to $a_{\pm}=-A_0\exp(\mp i\kappa_y y)\exp(i\varphi_{\pm})$ for $x\rightarrow+\infty$. Unfortunately, we failed to find an exact solution to (7) that would meet these conditions. One can derive an approximate solution to (7) by matching the solutions $a_{\pm}=A_{\pm}\exp(\pm i\kappa_y y)\exp(i\varphi_{\pm})$ and $a_{\pm}=A_{\pm}\exp(\mp i\kappa_y y)\exp(i\varphi_{\pm})$ at the points where $A_{+}=0$ and $A_{-}=0$. Note that only the individual phases φ_{+} and φ_{-} make a jump at the points of matching, whereas the solutions for $A_{\pm}$ and Φ remain smooth.

The proposed model predicting the existence of the domain wall is rather crude, of course. It does not take into consideration the effects associated with discrete position of the dislocations or the nonlinear damping which may be rather significant. However, this model accounts for the main effect of interest to us, i.e., for the parametric coupling of counterpropagating waves, and describes correctly the characteristic feature observed in the experiment, namely a double domain wall.

III. CONCLUSION

Experiments on investigation of the dislocations in parametrically excited capillary ripples demonstrate that their structure and dynamics differ greatly from the structure and dynamics of the dislocations observed at thermoconvection or at electrohydrodynamic convection in liquid crystals. This difference lies primarily in that each dislocation is a bound state of two topological defects of the same sign belonging to counterpropagating capillary waves. The stability of such a bound state is due to the parametric pump field.

The dynamics of dislocations in the capillary ripples consisting of two mutually orthogonal pairs of standing waves is significantly affected by weak interaction of the dislocations belonging to different pairs, whereas the dislocations belonging to the same pair interact effectively. They annihilate if they have opposite topological charges and may be self-organized in the form of a linear chain if they have like charges.

The results presented in this paper pose new questions. It is highly important to elucidate, for example, what determines the periodicity of dislocations in the domain wall shown in Fig. 7 and whether the effect of pinning exists in parametrically excited ripples when the position of dislocations is correlated with the wave phases in mutually orthogonal pairs.

ACKNOWLEDGMENTS

The authors are grateful to Professor M. I. Rabinovich for simulating discussions and constant interest in our investigations, as well as to Dr. L. N. Korzinov, Dr. K. A. Gorshkov, Dr. M. M. Sushchik, and Dr. V. P. Reutov for valuable comments. We also thank S. Kuznetsov for technical assistance. This work was carried out with the support of the Russian Foundation for Basic Research (Grant No. N 94-02-03263-a) and the International Science Foundation (Grant No. NOU000).

[1] S. Douardy and S. Fauve, Europhys. Lett. **6**, 221 (1988).
[2] W. S. Edwards and S. Fauve, Phys. Rev. E **47**, 788 (1993).
[3] B. Christiansen, P. Alstrom, and M. T. Levinsen, Phys. Rev. Lett. **68**, 2157 (1992).
[4] A. B. Ezersky, M. I. Rabinovich, V. P. Reutov, and I. M. Starobinets, Zh. Eksp. Teor. Fiz. **91**, 2070 (1986) [Sov. Phys. JETP **64**, 1228 (1986)].
[5] N. B. Tufillaro, R. Ramshankar, and J. P. Gollub, Phys. Rev. Lett. **62**, 422 (1989).
[6] A. B. Ezersky, S. V. Kiyashko, P. A. Matusov, and M. I. Rabinovich, Europhys. Lett. **26**, 183 (1994).
[7] S. Rasenat, V. Steinberg, and I. Rehberg, Phys. Rev. A **42**, 5998 (1990).
[8] A. Joets and R. Ribotta, in *Cellular Structures in Instabilities,* edited by J. F. Wesfreid and S. Zalesky, Lecture Notes in Physics Vol. 210 (Springer-Verlag, Berlin, 1984), p. 294.
[9] R. Ribotta and A. Joets, in *Cellular Structures in Instabilities* (Ref. [8]), p. 249.
[10] V. Croquette and A. Pocheau, in *Cellular Structures in Instabilities* (Ref. [8]), p. 104.
[11] J. A. Whitehead, Phys. Fluids **26**, 2899 (1983).

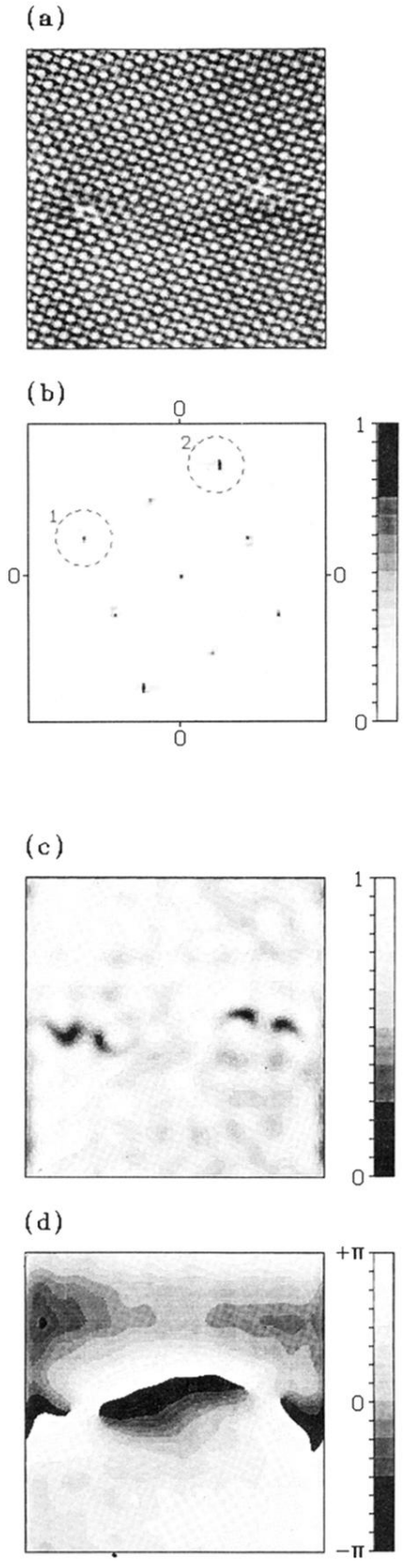

FIG. 2. (a) Field of capillary ripples. (b) Fourier spectrum. The dashed lines mark the spectral peaks for which the envelope fields were investigated. (c) Field of the amplitude of envelope for spectral peak 1. (d) Field of the phase of envelope for spectral peak 1.

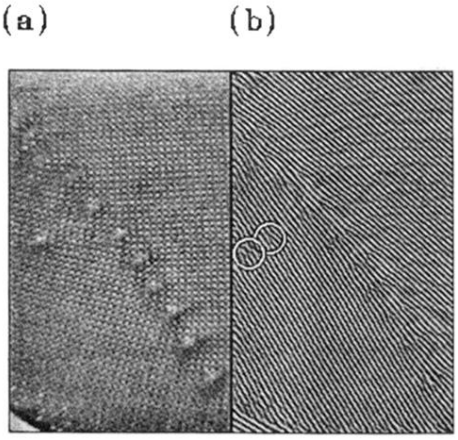

FIG. 6. Linear chain of dislocations for $\varepsilon = 0.47$ and $f = 102$ Hz: (a) image of capillary ripples; (b) filtered and contrasted image of a single wave pair.

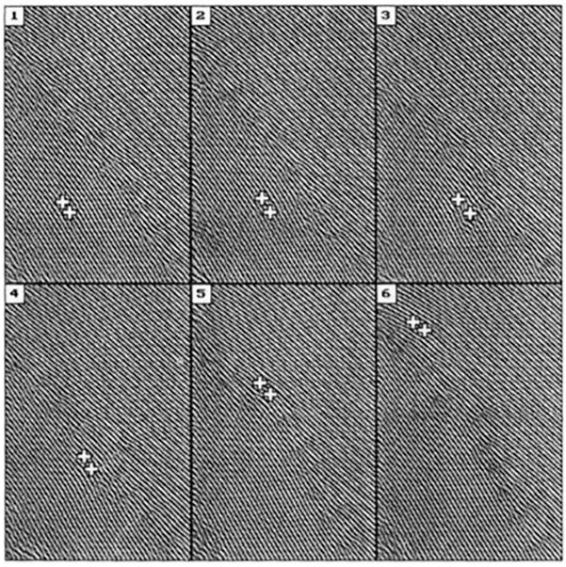

FIG. 7. Dislocations passing through the wall for $\varepsilon = 0.47$ and $f = 100$ Hz. Repetition rate for frames 1 and 2, 2 and 3 is 0.24 s, and for the other frames 0.12 s.